Fibers and Polymers 2020, Vol.21, No.8, 1832-1840
DOI 10.1007/s12221-020-9979-4

ISSN 1229-9197 (print version)
ISSN 1875-0052 (electronic version)

Polyurethane Foam Reinforced with Fibers Pineaplle Crown Biocomposites for Sorption of Vegetable Oil

Isabella Loureiro Muller Costa[1], Francisco Maciel Monticeli[2], and Daniella R. Mulinari[3]*

[1]*Department of Chemical and Materials Engineering, Pontifical Catholic University of Rio de Janeiro, Rio de Janeiro, RJ 22451-900, Brazil*
[2]*Department of Materials and Technology, Guaratinguetá School of Engineering, São Paulo State University (Unesp), Guaratinguetá 12516-410, Brazil*
[3]*Departament of Mechanical and Energy, Technology College, Universidade do Estado do Rio de Janeiro, Resende 27537-000, Brazil*

(Received September 12, 2019; Revised November 20, 2019; Accepted December 16, 2019)

Abstract: The concern in reducing the environmental impacts caused by human interference is increasing. Thus, the objective of this study was to generate a sustainable solution for sorption of vegetable oil. It was developed and characterized biocomposites obtained from polyurethane derived from castor oil reinforced with fibers from the crown of pineapple for sorption of vegetable oil. The biocomposites were obtained by mass mixing the polyol with the prepolymer (1:1) and reinforced with 5 to 20 % (wt/wt) pineapple crown fiber in 18 and 35 mesh granulometry. The biocomposites and pure polyurethane were characterized by scanning electron microscopy (SEM), optical microscopy (OM), X-ray Diffraction (XRD), porosimetry, contact angle, and density. Sorption tests were carried out on the biocomposites and pure polyurethane (PU). The sorption capacity of the biocomposites was evaluated as a function of the fiber content inserted in the matrix. Results of the sorption tests showed that the biocomposites reinforced with fibers of 18 mesh (20 % wt) presented approximately twice the sorption capacity when compared to pure PU and others biocomposites results, due to high porosity combined with high surface area, which influenced directly in the oil sorption. Response surface methodology (RSM) tecnique confirmed the influence fibers granulometry and content on oil sorption.

Keywords: Sorption, Vegetable oil, Biocomposites, Pineapple crown, Polyurethane

Introduction

In recent decades occurred an increase in awareness of environmental risks in the industrial activities associated with the oil production chain [1-3]. Fossil fuels and their by-products impede the aeration and natural lightening of watercourses, due to the formation of a film insoluble in the surface, which produces harmful effects to the fauna and flora [2].

Careful selection and appropriate use of equipment and materials for oil recovery and removal are required. Some strategies have been studied, such as: in situ firing, dispersants, floating barriers and sorbent materials [4,5]. In situ firing depends directly on the thickness of the spill and generates high air pollution during firing [4,6]. The dispersants present advantageous environmental results, however, they have a high application cost. The floating barriers are a method of containment, which dependent on a second methodology for recovery of the affected area [4].

The use of sorbent materials for remediation of areas affected by oil spills is one of the most studied methods, considering the cost benefit. Natural organic sorbents are those derived from sources of lignocellulosic origin, such as natural fibers [6-9]. In addition, these fibers have low production costs, are abundant raw materials, are environmentally friendly and have the capacity to absorb 3 to 15 times their weight in oil [2,8].

Polyurethane is an interesting material because it is a porous absorbent with a hydrophobic polymeric matrix that has polar functional groups, with excellent capacity to remove oils and fats [10-12]. Polyurethane resins derived from natural sources through biomonomers are obtained from renewable sources, e.g. castor oil, extracted from the seed of the *Ricinus Communis* plant, which can be found in subtropical regions mainly in Brazil [13,14].

The use of natural fibers as reinforcement in polyurethane foams produced a biocomposite with natural substrates, which partially confers certain biodegradability to the material in order to reduce the post-consumption environmental impact [15]. Among the various natural fibers, pineapple crown is a very abundant agro-industrial residue in Brazil and may have many more applications [16]. Pineapple leaf fiber (PALF) consists of cellulose about 70-80 % wt giving its high specific modulus and strength compared to others fibers [17,18].

Thus, the objective of this work was to evaluate the sorption capacity of vegetal oil in the polyurethane derived from castor oil reinforced with pineapple crown fiber biocomposites.

*Corresponding author: dmulinari@hotmail.com

Experimental

Materials

In order to obtain the biocomposites, pineapple crown fibers (collected at the Lorena-SP fair) and polyurethane (supplied by Polyurethane, located in Belo Horizonte - MG) were used Polyol derived from castor oil Biopol L40H and Biopol ISO MDI isocyanate were used to manufacture the polyurethane.

After collection, the pineapple crown was separated manually (Figure 1a) and dried at 100 °C for 24 hours (Figure 1b). Then, the fibers were crushed and sieved; only fibers, which passed through the 18 and 35 mesh sieves, were used. The pineapple crown fibers were studied without any chemical treatment or cleaning process. Only one type of oil was used: vegetable oil collected from local market.

Synthesis of Biocomposites and Polyurethane Foams

Pure polyurethane (PU) was synthesized with polyol and isocyanate (prepolymer) by mass mixing equal to 1:1. The mixture of the reagents was done manually; homogenization of the polyol with isocyanate occurred at room temperature, approximately 25 °C for 50 sec. After 24 hours, the PU was removed from the molds.

For synthesis of the polyurethane/fibers (pineapple crown) biocomposites, firstly fibers were mixed to the polyol and then the isocyanate was added. Biocomposites were synthesized with different total mass percentages (wt%) 5, 10 and 20 % of fibers, respectively for 18 and 35 mesh, with same parameters of the pure polyurethane (PU).

Figure 1. Pineapple crown; (a) Green (virgin) and (b) Dehydrated.

Characterization

To determine the apparent density was used the ASTM D 1622-14 standard, performed in triplicate. Morphology of the pure polyurethane, fibers and biocomposites were obtained in a scanning electron microscope HITACHI TM 3000 with tungsten filament operating at 15 kV, employing low-vacuum technique and secondary electron detector. Samples were dispersed on a brass support and fixed with a double face 3M tape. This analysis was used to determine the morphology of the materials, mainly to the aspects related to pores, such as size, quantity and geometry. The dispersion of the fibers in the biocomposites can be evidenced by optical microscopy technique (OM) using ZEISS Axio Imager 2.

Void volume fraction, diameter distribution and surface area were determined using mercury porosimetry equipment from Quantachrome Instruments®. Hg porosimetry was used with were 241 kPa of pressure, 20 s of dwell time and vacuum of 25 kPa. Parameters used were to ensure no compressibility in material during analysis.

The physical structures of the materials were evaluated by X-ray diffraction using a Shimadzu diffractometer, model XDR-6100. The measuring conditions were: CuKa radiation with graphite monochromator, 30 kV voltage and 40 mA electric current. The patterns were obtained in 10-50 ° angular intervals with 0.05 step and 1 s of counting time.

The contact angle was measured with a Ramé-Hart goniometer model 300-F1, carrying out DROP image Standard software. Therefore, five μ*l* droplets of the glycerine solution were deposited on the surface of each biocomposites.

Sorption Test

The method used for the measurement of vegetal oil sorption capacity of the sorbent was based in the research developed by Li, Liu and Yang [19].

The vegetal oil sorption capacity from pure PU and biocomposites was studied under a dynamic system. In the sorption tests, vegetal oil (75 m*l*) was poured into a 100 m*l* erlenmeyer flask. The sorbent was weighed and the value recorded, then it was immersed into the oil. The sealed flask was then placed in a shaker (40 rpm) and shaken for 1 hour to 48 hours. After 48 hours of immersion, the sorbent was removed and allowed to drain for 2 min. The saturated sorbent was then immediately transferred to a pre-weighed weighing bottle and weighed. The oil sorption of sorbent was calculated using the following equation:

$$\text{Oil sorption}\left(\frac{g}{g}\right) = \frac{M_f - M_i}{M_I} \times 100 \quad (1)$$

where, M_i is initial dry weight of sorbent and M_f is the weight of sorbent with oil absorbed, respectively. Pure polyurethane sorption capacity measurements were carried out similarly, in order to compare it with biocomposites results.

In water-oil system sorption tests, 4 g of vegetal oil was poured into a 100 m*l* erlenmeyer flask which was filled with 50 m*l* of deionized water. The sealed flask was then placed in a shaker (40 rpm) and shaken for 1 hour to 48 hours. The sorbent was removed and allowed to drain for 2 min, then immediately transferred to a pre-weighed weighing bottle and weighed. The oil sorption in water-oil system was calculated using the following equation:

$$\text{Oil sorption } \left(\frac{g}{g}\right) = \frac{S_f - S_i}{S_I} \times 100 \quad (2)$$

where, S_i is initial dry weight of sorbent and S_f is the weight of sorbent (after water sorption).

Results and Discussion

Properties of Used Oil

Table 1 evidences the physical-chemical properties obtained in the tests performed on vegetable oil which was used in the sorption test. Soybean oil has a slightly yellowish, clear color, with a characteristic mild odor and taste.

Density, SEM and OM

The addition of fibers to polyurethane, as well as, the fiber granulometry influenced directly on density of biocomposites, resulting in materials with the different pores volume. Figure 2 evidences the density obtained of biocomposites and pure polyurethane.

Table 1. Physical properties of vegetable oil

Oil characteristic	Value
Viscosity (cp)	88
Density ($g \cdot m^{-3}$)	92
Index of saponification (mg KOH g^{-1})	189-195
Refractive index (40 ºC)	1.466 a 1.470

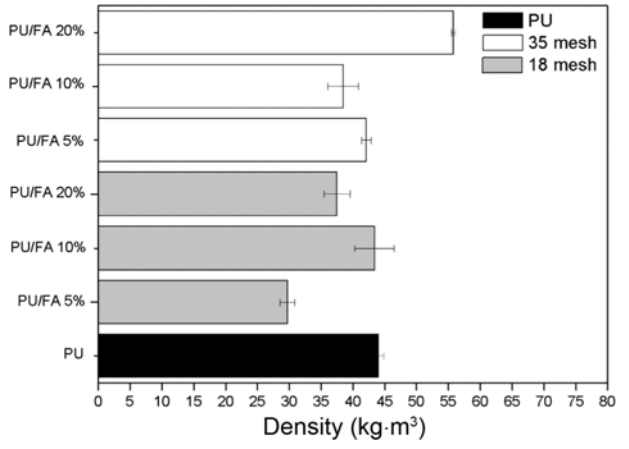

Figure 2. Density of the pure PU and biocomposites.

As the fiber content in the biocomposites increased, it was observed a variation in the density, which didn't occur gradually due to the non-uniformity of the fibers in the polyurethane, mainly in the case of fibers with higher grain size. It was observed that the greater deviations were found in the biocomposites reinforced with fibers in the 18 mesh sieve, which can be observed in Figure 2, because they have larger dimensions, which caused difficulty in mixing during the obtaining of biocomposites. Increasing the density of amorphous polymers generally decreases the diffusion coefficient due to the decrease in the free volume [20-22].

Tanobe *et al*. [2] carried out static and dynamic sorption tests on two polyurethane samples with different apparent densities, the lower density polyurethane had pores with larger diameters and smaller number of pores per cm^2, whereas the higher density polyurethane had higher numbers of pores per cm^2, and after the tests it was concluded that in short times what predominates in the rate of sorption is the area of pores, but in longer times is the quantity of pores present in the sorbent material.

The density results obtained in this study corroborate the morphology of biocomposites, pure polyurethane and fibers. The darkest regions are the interstitial spaces and the lightest

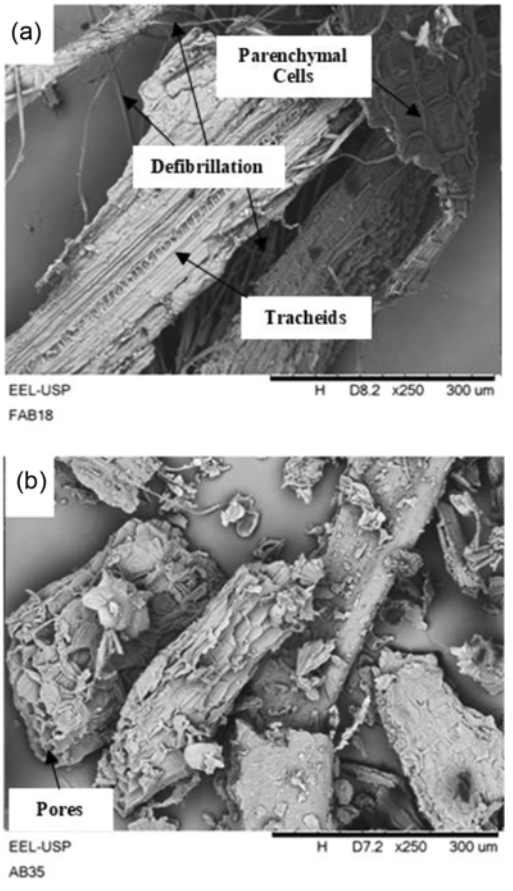

Figure 3. Fiber SEM images (250x); (a) 18 mesh and (b) 35 mesh.

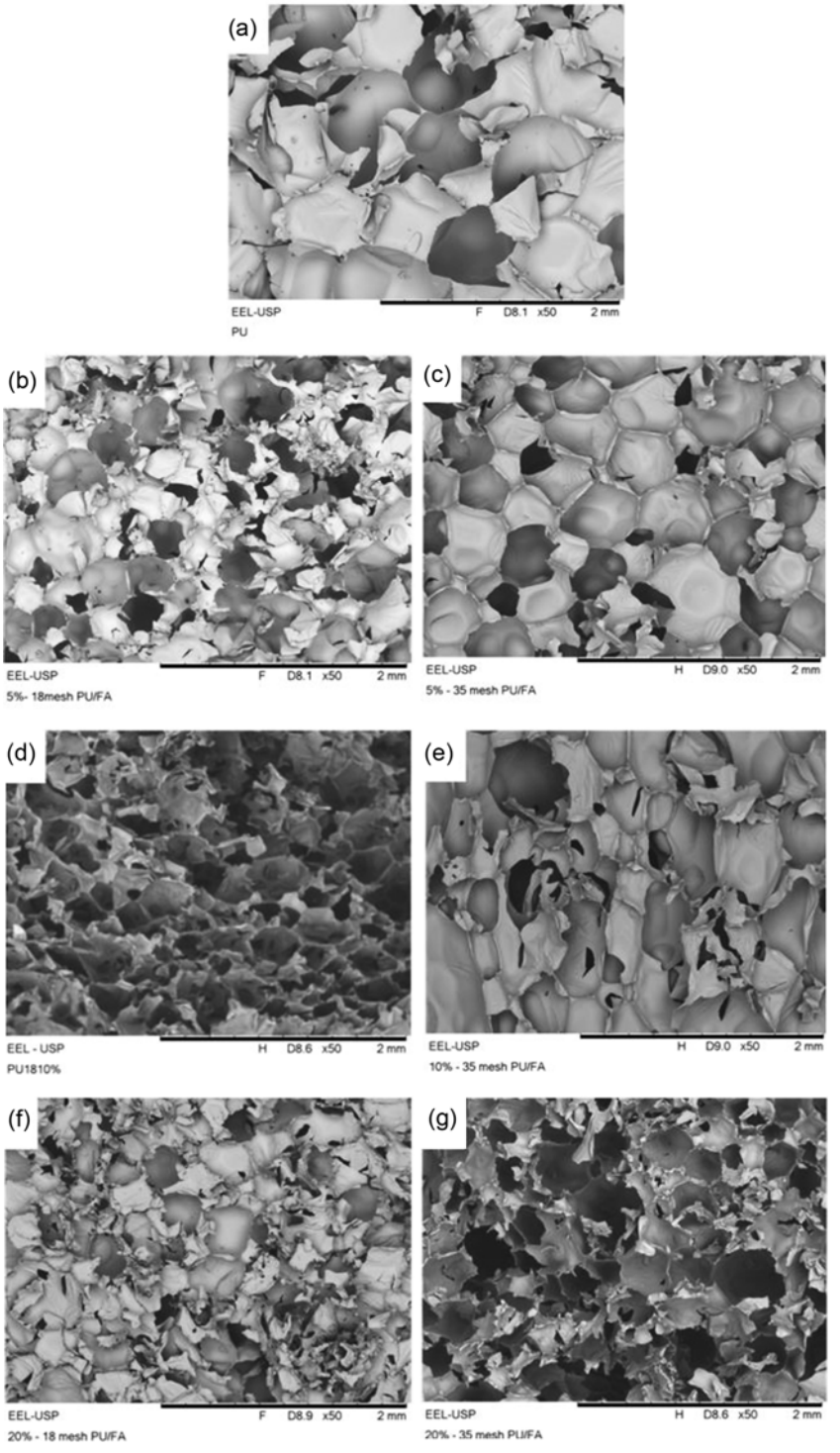

Figure 4. Materials SEM analysis (50x); (a) pure PU puro, (b) PU/FA (5 %) 18 mesh, (c) PU/FA (5 %) 35 mesh, (d) PU/FA (10 %) 18 mesh, (e) PU/FA (10 %) 35 mesh, (f) PU/FA (20 %) 18 mesh, and (g) PU/FA (20 %) 35 mesh.

regions represent the pore distribution, which occurred in a heterogeneous way. The lower the density of the foam, the larger the pore size. With the insertion of the fibers in the polyurethane the pore size decreased, consequently the pore volume increased, causing an increase in the density of biocomposites. A large difference in size, quantity and geometry was observed. All the samples presented a thin film, due to the expansion phase, classified as closed cells.

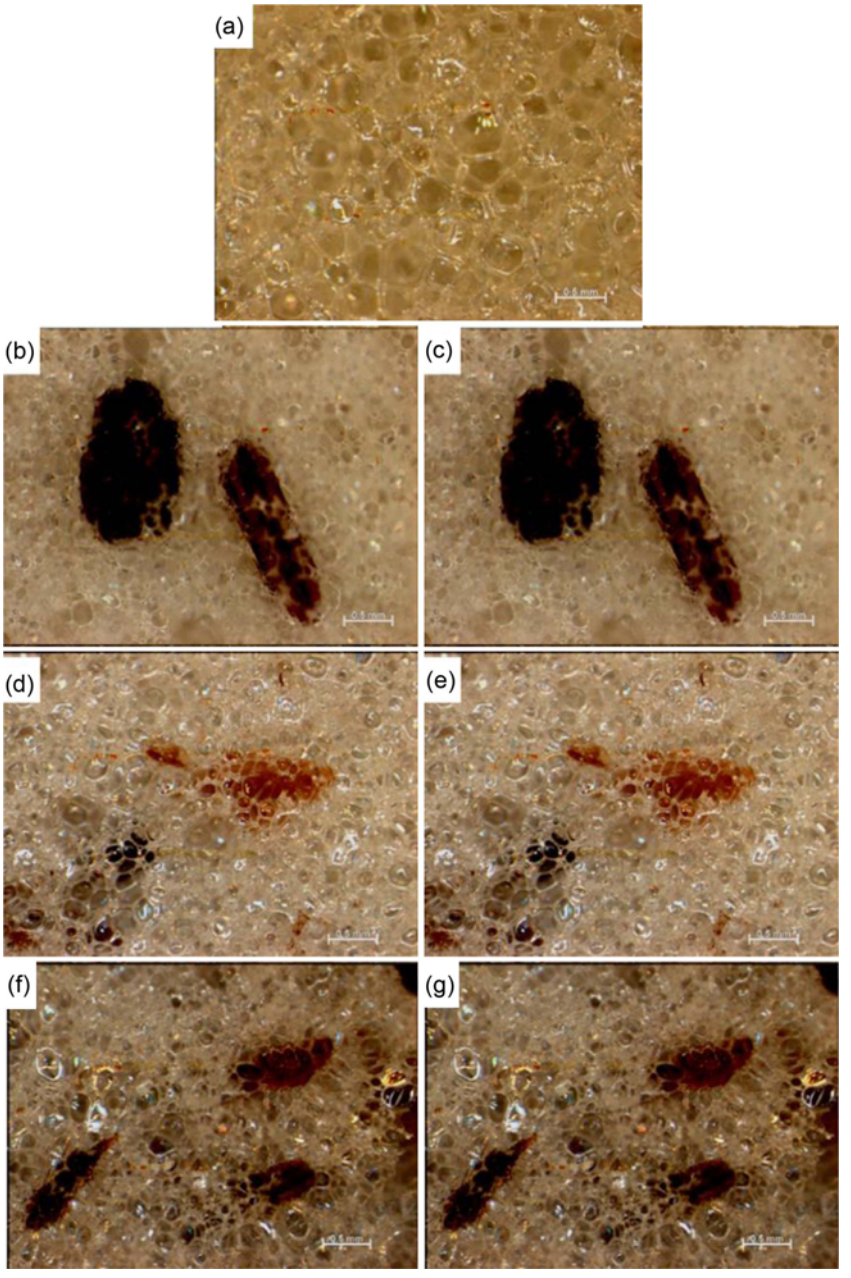

Figure 5. Microscopic images (30x): (a) pure PU, (b) PU/FA (5 %) 18 mesh, (c) PU/FA (5 %) 35 mesh, (d) PU/FA (10 %) 18 mesh, (e) PU/FA (10 %) 35 mesh, (f) PU/FA (20 %) 18 mesh, and (e) PU/FA (20 %) 35 mesh.

Figure 3 evidences a rough surface, presence of tracheid's, parenchyma cells and defibrillation caused by the crushing process, in which can increase the contact area and favor greater wettability between fiber and polymer.

The morphology of the pure polyurethane (Figure 4A) evidence a porous surface with darkest regions (interstitial spaces) and the lightest regions represent the pore distribution, which occurred in a heterogeneous way. The SEM images of the biocomposites show the formation of less homogeneous and more deformed cellular structure with the addition of fibers from pineapple crown (Figure 4). The fiber increases the surface area of the material, has internal pores that have smaller diameters and by capillary action can adsorb the oil, potentiating the sorption capacity of the polyurethane by the surface of contact with the oil.

Fiber pineapple addition results on voids increase per area and, consequently, a diameter reduction of porosity, mainly for specimens with 18 mesh of fibers. Biocomposites reinforced with 18 mesh of fibers (Figures 4b, 4d and 4f) shown higher porosity with smaller diameters compared

Table 2. Hg porosimetry result (void volume fraction)

Material	Fiber volume fraction (%)	Porosity fraction (%)	Surface area ($m^2 \cdot g^{-1}$)
Pure PU	-	50.77	1.52
18 mesh	5	42.60	1.23
	10	45.24	1.43
	20	67.47	3.22
35 mesh	5	57.14	1.49
	10	61.18	2.79
	20	66.13	3.01

with those fibers with 35 mesh (Figures 4c, 4e and 4g). Porosity and void diameter will be quantitatively discussed in Hg porosimetry results section. Bandegi *et al*. [23] observed a porous surface, presenting several types of pores, such as open pores, closed, in the form of transport cages, which give them great adsorption power.

Through the optical micrograph was possible to observe that in the biocomposites there are several types of pores, but the greater irregularity was found in the matrices reinforced with fibers of 18 mesh sieve (Figure 5).

The images obtained by optical micrograph technique showed the dispersion of fiber in the matrix of pure polyurethane and biocomposites, which was not feasible through the SEM micrographs (Figures 5b, 5d and 5f).

In addition to the effects of the pores, the images revealed that the particles are not arranged homogeneously. These particles have irregular shapes and a complex topographic surface, with many reentrant regions, which may influence their performance in removal oils [24].

Porosity, Contact Angle and XRD

Surface area is a crucial parameter in adsorption process. The technique of Hg porosimetry provided the measures of void volume fraction of each specimen, as well as BET surface area (S_{BET}) and voids diameter distribution. Table 2 presented porosity fraction and surface area, which both parameters are directly proportional to each other, considering that surface porosity will necessarily create more areas connected to surface [25].

Considering fiber volume fraction increase, porosity fraction and surface area tends to increase in each specimen. Specimens that presented higher porosity fraction and surface area compared with pure PU were: 18 mesh (20 %) and all specimens for 35 mesh. Fiber with larger mesh were susceptible to increases porosity (increasing surface area), which could make it difficult the PU formation during chemical link. However, 18 mesh, especially those with less fiber fraction decreases porosity, considering that with higher movement, lower fraction of small fibers agglutinated and avoid porosity, which detrimental for sorption characteristic.

According to the literature, loads in PU foams affect the walls of their cells, contributing to the rupture of their wall due to the destabilizing effect of the load through mechanisms of retraction of the edges of the cells, this explains the increase in porosity [1,2].

For a better porosity characterization, diameter distribution was carried out (Figure 6) from mercury intrusion method, which is one of the most traditional methods in determining the open pore size distribution and apparent porosity. In this method, mercury is injected into the sample and the pressure is increased during the process by simultaneously measuring

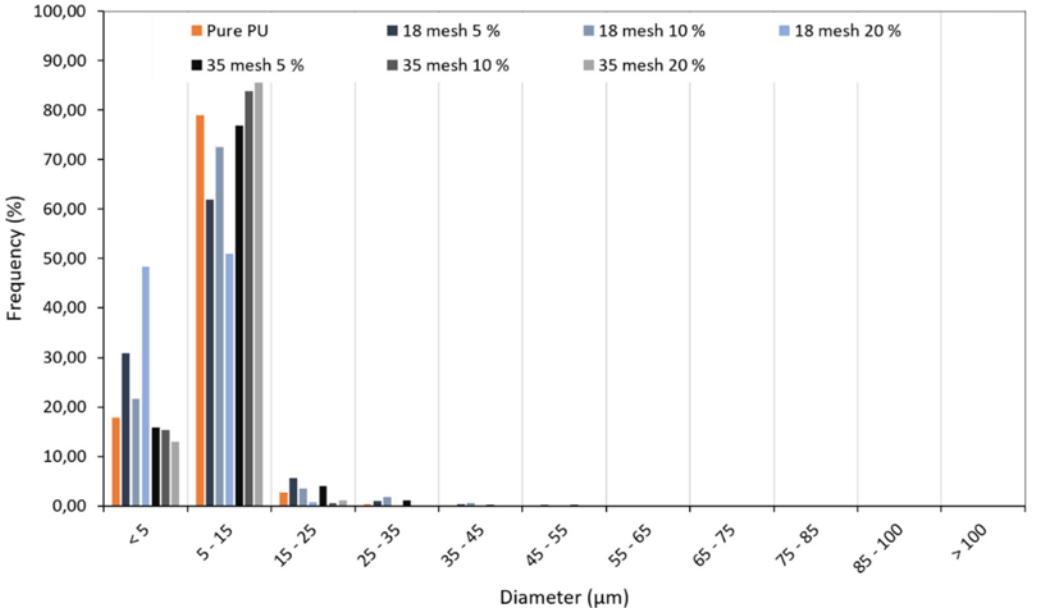

Figure 6. Void diameter distribution.

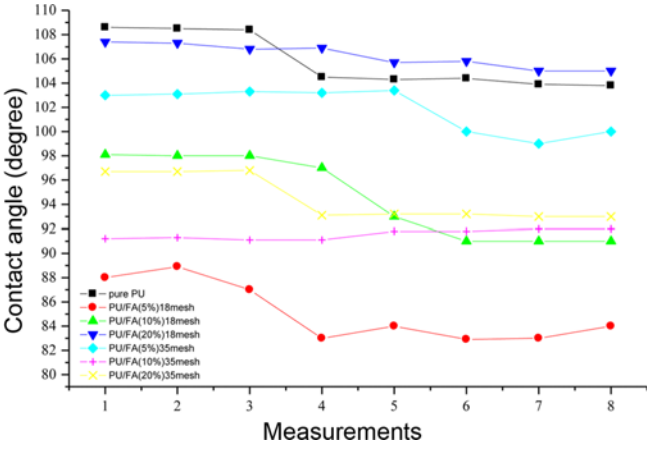

Figure 7. Measurements contact angle between water and the surface of the materials.

the volume of mercury introduced. The pore diameter of the part is related to the pressure required to inject the mercury [26]. The pressure and volume of mercury introduced were correlated in order to obtain the percentage porosity and the pore size distribution of the sample.

Void diameter range was 4.2-142 μm, in which porosity higher than 35 μm presented frequency less than 1 %, which was considered sporadic in all materials analyzed, indicating it is macroporous texture. In other hand, most frequency was found in the range 5-15 μm. Void diameters for pure PU and all biocomposites with 35 mesh of fibers presented same behavior, with same frequency in the range 5-15 μm (i.e., > 75 %) and, as consequence, smaller porosity (> 5 μm) with less frequency (i.e., up to 18 %).

Biocomposites reinforced with 18 mesh of fibers presented same behavior previous analyzed (Figures 4 and 5), in which it was more prone for smaller void formation. Biocomposites with 18 mesh (5 %) presented an increase in smaller void (>5 μm) frequency (i.e., 30 %). These behavior changes for 18 mesh (10 %), in which smaller porosity presented only 20 % of frequency. The biggest change occurred with 18 mesh (20 %), material which presented 48 % of smaller frequency, and 50 % of porosity in the range of 5-15 μm.

The fiber content presented an important factor in void amount and respective morphology. Greater fiber fraction inserted in biocomposites resulted in greater void formation. Regarding pore morphology, there is an ideal fiber addition proportion to increase void content and control morphology. Biocomposites reinforced with fibers 18 mesh (PU/20 % wt) indicated higher porosity with small diameter, which could be an important factor to increase capillary effect and, consequently, increase sorption characteristics [27,28].

Figure 7 shows the measurements obtained of the contact angle (CA) of the materials. This technique was used to analyze the behavior of different fibers concentrations on pure polyurethane. It was noted during measurements

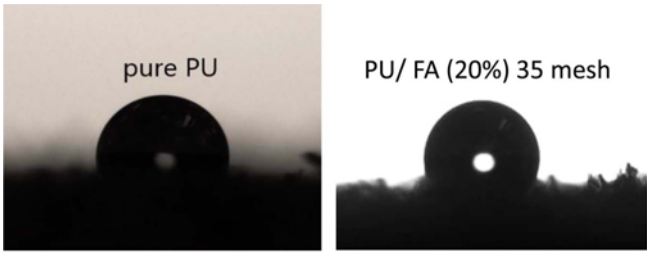

Figure 8. Images of water droplet in contact with the surface of the materials.

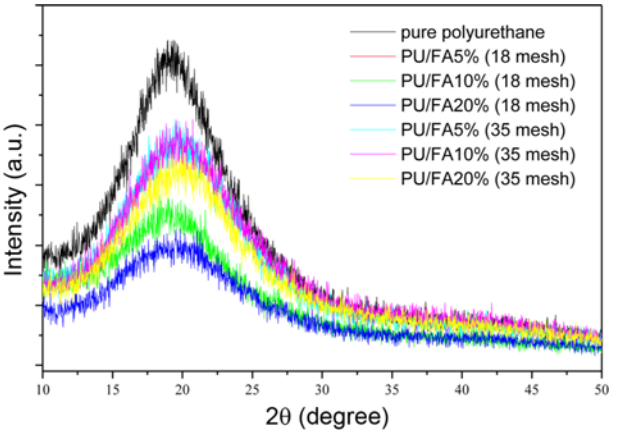

Figure 9. XRD spectra of pure polyurethane and biocomposites.

between the pure polyurethane and water a reduction in the CA value of 109 ° to 105 °, characteristic values of hydrophobic material. However, when adding fibers in the polyurethane matrix a reduction of the contact angle (CA) was observed. Santos *et al*., cited that, when the surface energy is lowered, the hydrophobicity of the material is enhanced [28,29]. The increase in surface polyurethane foam hydrophobicity increases the oil sorption capacity [29].

Biocomposites reinforced with 18 mesh of fibers (PU/ 20 % wt) evidenced measurement's contact angle next to pure PU (Figure 8), guaranteeing even greater hydrophobicity to the material and, consequently, greater sorption capacity of oil. The difference in granulometry influenced these results.

In order to investigate the crystalline structure of pure polyurethane and biocomposites, XRD spectra were studied as shown in Figure 9.

It was observed that crystalline structure of biocomposites was decreased by addition of fibers in the pure polyurethane. The characteristics peaks were at 18 to 19 ° in all materials as shown in Figure 9, representing the characteristic peak of segmented polyurethane [30]. The intensity of these peaks also was decreased with the increase of the fibers content in the polyurethane, studied XRD spectra of biocomposites. These results obtained by characterization techniques

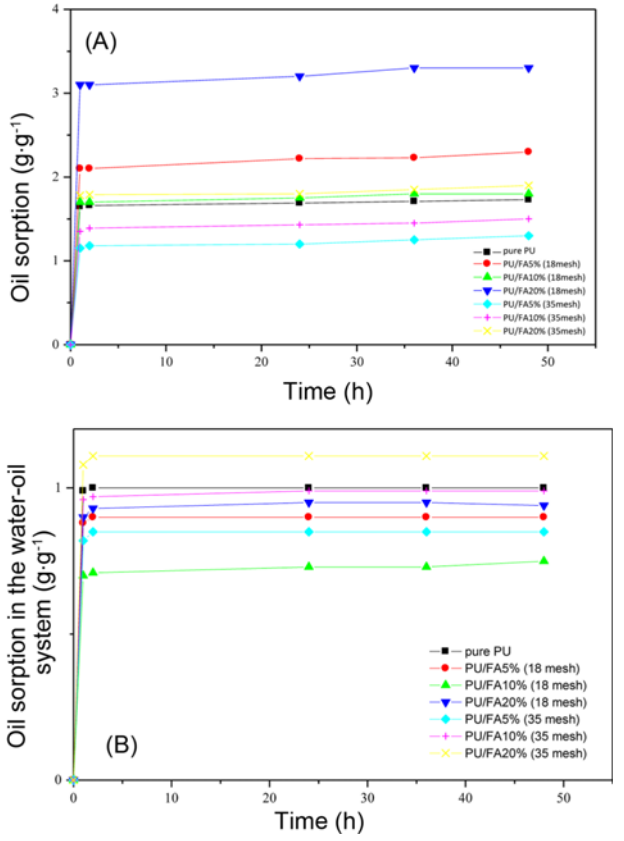

Figure 10. Oil sorption capacity of the pure PU and biocomposites as a function of time in oil system (A) and in water-oil system (B).

corroborate with the results of vegetal oil sorption in the materials.

Sorption Results

The Figure 10 shows the vegetal oil and oil and water system as function of time sorption capacities of the pure polyurethane and biocomposites.

All materials showed a higher oil sorption capacity in the oil system compared to water-oil system after contact time of 48 hours. This result corroborates with contact angle results, indicating that biocomposites reinforced with 18 mesh of fibers (PU/20 % wt) evidenced greater hydrophobicity to the material and, consequently, greater sorption capacity of oil when compared to the pure PU and biocomposites. Fibers reduce the hydrophobic character of pure polyurethane due to the polar groups in the structure, which can favor the sorption of organic compounds [29]. The proposed materials presented lower sorption capacity when compared to the palm fibers used as adsorbents for vegetable oil. This difference can be explained by the fact that the density and viscosity of the vegetable oil used in this work is smaller, because the higher the viscosity, the slower the fluid will move [31].

On the other hand, results of sorption of the biocomposites

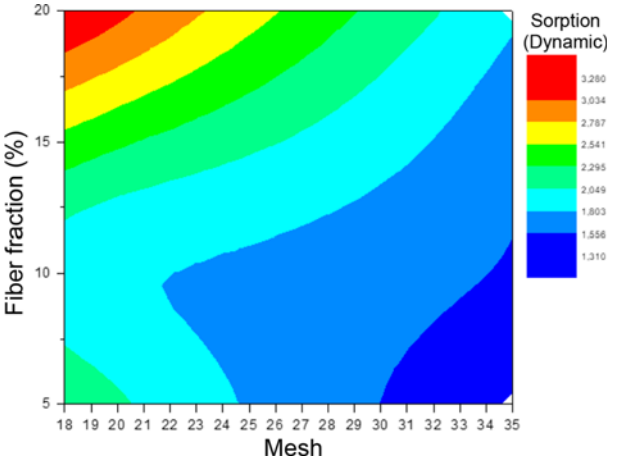

Figure 11. Surface response for dynamic oil sorption.

reinforced with fibers of 18 mesh granulometry showed an interesting variation, in which sorption capacity presented a decrease in intermediate fiber fraction (10 % wt). This result was related to void diameter distribution, in which the increase of smaller diameters created a capillary force between porosity that resulted in higher sorption capacity. Results in which it was possible to conclude a linear dependency on smaller void formation for a better sorption capacity, in which there is an appropriated number of reinforcements to ensure small void morphology.

Response surface methodology (RSM) technique was applied for oil sorption. RSM was used to determine statically the appropriated material for higher sorption capacity (shown in legend of Figure 11). It was possible to observe a tendency in sorption capacity: higher fiber fraction combined with lower mesh resulted in higher sorption results, as well as the decrease of fiber fraction combined with higher mesh decreases sorption capacity.

Biocomposites reinforced with fibers of 18 mesh granulometry (20 % wt) combination resulted in higher porosity fraction and 48 % of porosity diameters less than 5 μm, consequently higher surface area with hydrophobic characteristics are the essential parameters to ensure Figure 11 results with maximal sorption capacity.

Conclusion

Pure PU and biocomposites (fibers reinforced in the polyurethane with different particle size) were used as sorbents for vegetal oil. The sorption capacity of materials was found to increase with time. The formation of a pore size hydrophobic material with small pore size was essential to physically analyze the results. Addition of larger (35 mesh) fibers in the biocomposites restricted the formation of void content and respective smaller void diameters (< 5 μm), which was detrimental to sorption capacity. On the other

hand, the use of fiber content with smaller sizes (18 mesh) allowed the formation of small pores added to the hydrophobic character of the material, in all cases increased the sorption capacity. Therefore, the biocomposites reinforced with fibers of 18 mesh (20 % wt) are the most suitable combination for oil sorption applications when compared to pure PU results.

Acknowledgement

Authors are grateful for the research support by FAPERJ (process E-26/010.002016/2014 and E-26/201.481/2014).

References

1. C. C. Schmitt, C. I. Yamamoto, E. V. Takeshita, V. O. A. Tanobe, and S. S. X. Chiaro, *J. Clean Prod.*, **140**, 1465 (2017).
2. V. O. A. Tanobe, T. H. D. Sydenstricker, S. C. Amico, J. V. C. Vargas, and S. F. Zawadzki, *J. Appl. Polym. Sci.,* **111**, 1842 (2009).
3. V. O. A. Tanobe, T. H. D. Sydenstricker, M. Munaro, and S. C. Amico, *Polym. Test.*, **24**, 474 (2005).
4. M. F. Fingas, *Int. Oil Spill Conf. Proc*., **1999**, 281 (2013).
5. J. P. Wilkinson, T. Boyd, B. Hagen, T. Maksym, S. Pegau, C. Roman, H. Singh, and L. Zabilansky, *Cold Reg. Sci. Technol*., **109**, 9 (2015).
6. A. A. Al-Majed, A. R. Adebayo, and M. E. Hossain, *J. Environ. Manage*, **113**, 213 (2012).
7. M. Adebajo, R. L. Frost, T. Kloprogge, and O. Carmody, *J. Porous Mater*., **10**, 159 (2003).
8. N. Baig, F. I. Alghunaimi, H. S. Dossary, and T. A. Saleh, *Process. Saf. Environ. Prot*., **123**, 327 (2019).
9. X. Zhang, F. Fu, X. Gao, and X. Hou, *J. Bionic. Eng*., **16**, 38 (2019).
10. B. R. Fenner, M. V. G. Zimmermann, M. P. Silva, and A. J. Zattera, *J. Mol. Liq*., **271**, 74 (2018).
11. C. Xia, Y. Li, T. Fei, and W. Gong, *Chem. Eng. J.,* **345**, 648 (2018).
12. J. Braun, M. O. Klein, J. Bernarding, M. B. Leitner, and H. D. Mika, *Polym. Test*., **22**, 761 (2003).
13. G. Trovati, M. V. N. Suman, E. A. Sanches, P. H. Campelo, R. B. Neto, S. C. Neto, and L. R. Trovat, *Polym. Test.*, **73**, 87 (2019).
14. T. P. T. Sousa, M. S. T. Costa, R. Guilherme, W. Orcini, L. A. Holgado, E. M. V. Silveira, O. Tavano, A. G. Magdalena, S. A. Catanzaro-Guimarães, and A. Kinoshita, *Polímeros*, **28**, 246 (2018).
15. O. S. H. Santos, M. C. Silva, V. R. Silva, W. N. Mussel, and M. I. Yoshida, *J. Hazard Mater*., **324**, 406 (2017).
16. K. S. Prado and M. A. S. Spinacé, *Mat. Res*., **18**, 530 (2015).
17. M. H. Zin, K. Abdam, N. Mazean, E. S. Zainudin, K. E. Liew, and M. N. Norizan, *Compos. Part B-Eng.*, **177**, 107306 (2019).
18. S. S. Todkar and S. A. Patil, *Compos. Part B-Eng.*, **174**, 106927 (2019).
19. H. Li, L. Liu, and F. Yang, *Mar. Pollut. Bull*., **64**, 1648 (2012).
20. B. Ghalei, A. P. Isfahani, M. Sadeghi, E. Vakili, and A. Jalili, *Polym. Adv. Technol.*, **29**, 874 (2018).
21. D. Hu, L. Zhao, L. Yan, T. Liu, and Z. Xu, *J. Appl. Polym. Sci*., **136**, 47100 (2018).
22. Z. F. Wang, B. Wang, Y. R. Yang, and C. P. Hu, *Eur. Polym. J*., **39**, 2345 (2003).
23. A. Bandegi and M. R. Moghbeli, *J. Appl. Polym. Sci*., **135**, 45586 (2018).
24. D. P. Queiroz, A. M. B. Rego, and M. N. Pinho, *J. Memb. Sci.*, **281**, 239 (2006).
25. C. Zhang, R. Kong, X. Wang, Y. Xu, F. Wang, W. Ren, Y. Wang, F. Su, and J. Jiang, *Carbon*, **114**, 608 (2017).
26. H. Gao, T. Li, and L. Yang, *J. Petrol. Explor Prod. Technol*., **6**, 309 (2016).
27. J. O. Alvarez, I. W. R. Saputra, and D. S. Schechter, *SPE J*., **23**, 2103 (2018).
28. Y. Shen, H. Ge, M. Meng, Z. Jiang, and X. Yang, *Energy and Fuels*, **31**, 4973 (2017).
29. J. Wang and G. Geng, *Mar. Pollut. Bull*., **97**, 118 (2015).
30. W. Lei, C. Fang, X. Zhou, Y. Li, and M. Pu, *Carbohydr. Polym*., **197**, 385 (2018).
31. O. Abdelwahab, S. M. Nasr, and W. M. Thabet, *Alexandria Eng. J*., **56**, 749 (2017).